Evaluation of Normal Tissue Complication Probability and Risk of Second Primary Cancer in Prostate Radiotherapy

Rungdham Takam

Thesis submitted for the degree of
Doctor of Philosophy
in
The School of Chemistry and Physics,
The University of Adelaide

Supervisors
A/Prof. Eva Bezak
Prof. Eric E. Yeoh
Dr. Guilin Liu

April 2010

Chapter 1

Introduction

1.1 Prostate cancer and radiotherapy

Prostate cancer is presently recognized as one of the major medical problems facing the male population (Aus *et al* 2005). It is also the second most lethal tumour among men (Cooperberg *et al* 2005). However, prostate cancer is a curable disease when it is diagnosed and treated at early stages.

There are varieties of treatment options available for prostate cancer, i.e. watchful waiting, radical prostatectomy, radiotherapy, hormonal therapy, and combined-modality treatment. Among all treatment options, number of men undergoing radiotherapy for prostate cancer is continuously increasing (Brenner 2000). Commonly, radiotherapy may be categorized into two main groups: (1) External

Beam Radiotherapy (EBRT) including Three-Dimensional Conformal Radiotherapy (3D-CRT) and Intensity Modulated Radiotherapy (IMRT); and (2) Brachytherapy (BT) including Low-Dose-Rate (LDR) and High-Dose-Rate (HDR) brachytherapy. The purpose of radiotherapy is to eradicate the cancerous cells while causing as little damage as possible to normal organs/tissues – this can be regarded as the ultimate goal of radiotherapy. Introduction of three-dimensional treatment planning has changed radiation therapy delivery capabilities dramatically and this change continues rapidly in response to the implementation of new advanced technologies (Purdy 2008). The modern radiation therapy modalities based on three-dimensional planning provide better target coverage and lower collateral doses to surrounding normal structures in comparison to early two-dimensional radiotherapy techniques.

As a result of introduction of extensive screening programs, more men of younger ages are being diagnosed with prostate cancer and radiotherapy may be recommended for the treatment of their disease. With advanced modern radiation treatment techniques and improved management of radiation-associated complications, the survival outcomes of prostate patients treated with radiotherapy are significantly improved. However, the achievement of improved cancer control has come with the growing concerns about the risk of late organs/tissues complications and radiation-induced carcinogenesis among the radiation-treated cancer survivors who are now younger and living longer (Xu *et al* 2008). Therefore, there is a need to evaluate carefully the radiation treatment plans that are to be used clinically to determine the radiation-associated Normal Tissue Complication Probability (NTCP) and the risk of development of Second

Primary Cancer (SPC). These evaluations have become important issues which can assist the radiation oncologists and the patients in decision making regarding suitable radiation treatment technique for, in this thesis, the prostate cancer.

1.2 Evaluation of radiation treatment plans

There are two major components required in an evaluation of a radiation treatment plan; from the normal tissue injury perspective: (i) radiation dosimetric data representing the distributions of doses over the volume of an organ/tissue of interest, and (ii) appropriate radiobiological model which can be used to analyze the radiation dosimetric data to perform the evaluation (NTCP/Risk of SPC). The first component may be obtained directly from treatment plans in the form of Dose-Volume Histograms (DVHs) of normal organs. The physical dose based DVHs retrieved from the treatment plans may need to be transformed into a specific format to allow for application of a designated model and to make comparisons between different treatment plans corresponding to various radiotherapy techniques.

The second component requires the availability of NTCP or risk of SPC models which are applied to dosimetric data to compute the probability of normal tissue complications and risk of developing radiation-induced cancer, respectively. There are several models available. Majority of these models have been developed based on collective results of various epidemiologic retrospective studies conducted with a large group of cohorts. In addition, it is also possible to develop a model derived from the radiobiological data obtained from the clinical observations of a selected group of patients. In this thesis, the standard Lyman's (Lyman 1985 and Lyman &

Wolbarst 1987) and the relative seriality models (Kallman *et al* 1992, MacKay *et al* 1997, and Zaider *et al* 2005) were used to calculate NTCP whilst the competitive risk model (Gray 1965 and Dasu *et al* 2005) was used to estimate SPC.

In this thesis, a large number of DVHs (223 in total from 101 patients) of different plans from various radiotherapy treatment techniques for prostate cancer have been analyzed for both radiation-associated NTCP and risk of SPC. This study will demonstrate the methods of using DVHs and radiobiological models to evaluate the prostate radiation treatment plans of some older and some currently available radiation therapy techniques at the Royal Adelaide Hospital, South Australia.

It is well acknowledged that irradiation of the prostate using linear accelerator (linac) at treatment energy at or above 10 MV is associated with production of secondary neutrons in addition to leakage photons. Patient's whole body, outside the target region will be exposed to these radiations and there is a possibility that the radiation dose received might contribute to development of radiation-induced second cancer in the affected organs. Therefore, it is necessary to estimate the risk of SPC for the organs located beyond the prostate Planning Treatment Volume (PTV). However, DVHs of the organs located outside the PTV, i.e. liver, stomach, lungs, and thyroid, are not normally available for risk assessment using this approach. There is a need to evaluate the dose to the patient from secondary radiations (peripheral dose) by means of radiation dose measurement in the anthropomorphic Rando phantom irradiated to prostate External Beam Radiotherapy (EBRT) delivered by high-energy (>10 MV) linac. The results of this peripheral dose measurement will enable evaluation of the risk of SPC in the irradiated distant organs. There have been several reports published on the

determination of out-of-field or peripheral doses measured in a water phantom at different positions relative to the high-dose region or relative to the edge of the accelerator collimator (Xu *et al* 2008). However, measurements of photon and neutron peripheral doses in the Rando phantom are challenging because of technical difficulties in finding the dosimeters which can be placed inside the phantom slices and can measure photon and neutron doses simultaneously. These problems can be solved by using glass-rod ^{6}LiF:Mg,Cu,P and ^{7}LiF:Mg,Cu,P thermoluminescence dosimeters (TLDs). Both ^{6}LiF:Mg,Cu,P and ^{7}LiF:Mg,Cu,P TLDs have small sizes and sensitive to neutrons and photons, respectively. These TLDs can be fitted inside the Rando phantom allowing photon and neutron doses to be measured simultaneously and to enable evaluation of the radiation-induced carcinogenesis in the distant organs.

Therefore, the aims of this thesis are:

(1) To evaluate the radiation treatment plans of various radiotherapy techniques including 4-field standard fractionated (2 Gy/fraction to total dose of 64 Gy) and 4-field hypofractionated (2.75 Gy/fraction to total dose of 55 Gy) Three-Dimensional Conformal Radiotherapy (3D-CRT), 4-field dose-escalated 3D-CRT (to total dose of 70 or 74 Gy at 2 Gy/fraction), 5-field 3D-CRT (to total dose of 70 Gy at 2 Gy/fraction), Low-Dose-Rate Brachytherapy (LDR-BT) using I-125, High-Dose-Rate Brachytherapy (HDR-BT) using Ir-192, and combined-modality (3D-CRT and HDR-BT) treatment for localized prostate cancer using Dose-Volume Histograms (DVHs) and corresponding radiobiological models;

(2) To compare various radiation therapy techniques for prostate cancer in terms of associated Normal Tissue Complication Probability (NTCP) using the relative seriality and Lyman's NTCP models and risk of Second Primary Cancer (SPC) using the competitive risk model; and

(3) To develop a radiation dosimetry technique which enables measuring of free-in-air and in-phantom peripheral photon as well as neutron doses resulting from the prostate cancer irradiation using 3D-CRT with high-energy (>10 MV) medical linear accelerator and estimate the associated risk of second primary cancer in the affected organs/tissues.

1.3 Thesis outline

Chapter 1 introduces the importance of prostate radiation treatment plan evaluation and gives the objectives of this thesis.

Chapter 2 provides the general information about the prostate cancer, Treatment Control Probability (TCP), Normal Tissue Complication Probability (NTCP), and risk of developing Second Primary Cancer (SPC). Treatment techniques for prostate cancer are discussed briefly in this chapter.

Chapter 3 provides a review of NTCP models, Dose-Volume Histograms (DVHs), and methods of DVHs transformation to accommodate for differences in radiation treatment modalities and fractionation schedules.

Chapter 4 describes (in detail) the prostate cancer radiotherapy techniques involved in this study and their associated DVHs of normal organs/tissues of interest. The treatment plan evaluation results in terms of NTCP are presented and

discussed including testing of the result dependence on the variable model parameters.

Chapter 5 describes evaluation of the prostate radiation treatment plans in terms of the risk of radiation-induced SPC of the organs/tissues of interest which are normally irradiated to high radiation doses from the prostate cancer radiotherapy. The basis of the competitive risk model is introduced and the results of risk assessment are presented and discussed.

Chapter 6 introduces the general properties of novel ^{6}LiF:Mg,Cu,P and ^{7}LiF:Mg,Cu,P glass-rod thermoluminescence dosimeters (TLDs). The calibration methods for these TLDs are also provided. The results of the TLDs calibration and ambient out-of-field photon and neutron radiations measurements are presented and discussed.

Chapter 7 describes the importance of measuring peripheral radiation doses resulting from the prostate cancer irradiations. The use of ^{6}LiF:Mg,Cu,P and ^{7}LiF:Mg,Cu,P glass-rod TLDs in peripheral dose measurements with the anthropomorphic Rando phantom as well as approximations of distal organs/tissues doses are introduced. The peripheral doses in organs/tissues located away from Planning Treatment Volume (PTV) and associated risks of SPC are finally presented and discussed.

Chapter 8 presents the conclusions of this thesis.

Chapter 2

Introduction to prostate cancer and radiation treatment techniques

2.1 Prostate cancer

Prostate cancer is an abnormal and uncontrolled growth of cells originating in the prostate gland (Zeller 2007). In almost every patient, spread of cancer will have occurred along the perineural spaces within the gland. Cancer of the prostate gland is almost exclusively adenocarcinoma but transitional cell carcinoma may occur in the larger prostatic ducts (Moss *et al* 1973). In addition, nearly all cancers of the prostate originate in the peripheral parts of the gland or in the subcapsular zone. Prostate carcinoma is the most commonly diagnosed cancer in American men and is among the most common cancers diagnosed in many developed countries (Giovannucci & Platz 2006). In the United States, 234,460 new cases of prostate

cancer are expected to be diagnosed and 27,350 deaths from this disease are estimated in 2006 (American Cancer Society 2006). In Australia, it has become the major cancer affecting males accounting for over 29% (16,349 cases) of all invasive cancer diagnoses (56,158 cases) in 2005 (AIHW & AACR 2008).

2.1.1 Risk factors

Several factors have been implicated in the risk of developing prostate cancer but few of them have been identified. Age is the strongest risk factor for prostate cancer with the incidence of the disease increasing with advancing years (Aus *et al* 2005). Prostate cancer is rarely diagnosed in men aged less than 40 years old. In contrast, men aged between 75 and 79 have more than 100 times higher the risk of prostate cancer than those aged between 45 and 49 (Bishop 2003). It is therefore not surprising that the majority of men diagnosed with prostate cancer have been reported to be older than 65 years of age and that this age group accounts for the vast majority of deaths from prostate cancer (Giovannucci & Platz 2006).

Race is also one of the well-recognized risk factors for this disease. In United States, African-Americans have been reported to the highest incidence and mortality rates of prostate cancer, these being 275.3 per 100,000 men and 75.1 per 100,000 men annually during 1992 – 1999 respectively. Compared to white Americans, African-Americans have a 1.6-fold higher incidence rate and a 2.3 times greater mortality rate of prostate cancer.

Heredity is also a major risk factor. The relationship between family history and prostate cancer has been confirmed in population-based case-control, record linkage, and prospective cohort studies (Giovannucci & Platz 2006). These studies

found that in general, men with either a father or a brother with the diagnosis of prostate cancer are at approximately two to three times greater risk of developing prostate cancer than men without a family history of the disease.

Associations between prostate cancer incidence and consumption of fat, fruit and vegetables, alcohol and smoking have also been identified in some case-control studies but the results were inconsistent (Bishop 2003). Risk of prostate cancer in association with some occupations such as coal miners, chemists, French polishers and engine drivers have been reported but these have been no agreement in the results except for agricultural field workers involved in spraying herbicides. Links between hormones, sexual activity, marital status, and body mass index and incidence of prostate cancer have also been investigated but with varying results and no clear trends emerging.

2.1.2 Staging system for prostate cancer

Credit for categorizing prostate cancer in its various stages is due to Whitmore (1956) who proposed four stages of the disease (Miller & Montie 2006):

A. Clinically latent prostate cancer
B. Clinically manifested early prostate cancer
C. Clinically manifested locally advanced prostate cancer
D. Clinically manifested advanced prostate cancer with evidence of distant metastases.

However, the Whitmore staging system was replaced by the Tumour, Nodes, Metastasis (TMN) staging system (American Joint Committee on Cancer

(AJCC)/International Union Against Cancer (UICC)) in 1997, and the most recent update of the latter system being in 2003 (Table 2.1).

Table 2.1. *AJCC/UICC TNM staging system for prostate cancer (Zelefsky et al 2004).*

Primary tumour (T)	
TX	Primary tumour cannot be assessed
T0	No evidence of primary tumour
T1	Clinically inapparent tumour neither palpable nor visible by imaging
T1a	Tumour incidental histologic finding in 5% or less of tissue resected
T1b	Tumour incidental histologic finding in more than 5% of tissue resected
T1c	Tumour identified by needle biopsy (e.g., because of elevated prostate-specific-antigen)
T2	Tumour confined within prostate
T2a	Tumour involves one lobe
T2b	Tumour involves more than half of a lobe but not both lobes
T2c	Tumour involves both lobes
T3	Tumour extends through the prostate capsule
T3a	Extracapsular extension
T3b	Tumour invades seminal vesicle(s)
T4	Tumour is fixed or invades adjacent structures other than seminal vesicles
T4a	Tumour invades bladder neck, external sphincter, or rectum
T4b	Tumour invades levator muscles or is fixed to pelvic wall, or both
Regional lymph nodes (N)	
NX	Regional lymph nodes cannot be assessed
N0	No regional node metastasis
N1	Metastasis in single lymph node, 2 cm or less
N2	Metastasis in a single node, more than 2 cm but not more than 5 cm
N3	Metastasis in a node more than 5 cm
Distant metastasis (M)	
MX	Presence of metastasis cannot be assessed
M0	No distant metastasis
M1	Distant metastasis
M1a	Nonregional lymph node(s)
M1b	Metastasis in bone(s)
M1c	Metastasis in other site(s)

2.1.3 Treatment options for prostate cancer

Decisions regarding treatment for prostate cancer depend on a number of factors such as age, life expectancy, overall health status, Prostate Specific Antigen (PSA) level, Gleason score, and the growth and spread of the tumour (Zeller 2007). For a patient who has small volume and low-grade cancer with excellent prognosis, active monitoring in which the patient will receive regular check-ups and active treatment is deferred until the PSA level rises substantially or until symptoms appear may be appropriate (Shipley *et al* 2006). With this option, the patient has the benefit of avoiding the risks of overtreatment and side effects of treatment, sometimes severe. Active monitoring also has no effect on work or social activities of the patient. In the randomized trial comparing radical prostatectomy with watchful waiting in early stage prostate cancer reported by Holmberg *et al* (2002), radical prostatectomy significantly reduced disease-specific mortality but not overall survival compared with watchful waiting. However, many patients in this study did not have small volume, low grade cancer. The advantages of active monitoring as described above are therefore even more likely to outweigh the risks of immediate treatment in patients with small volume, low grade early stage prostate cancer. The risks of deferring treatment for other sub-groups of early stage prostate cancer, which include tumour progression beyond being curable at all or being curable at the cost of severe side effects resulting in death or serious patient morbidity are greater and more careful selection of patients for watchful waiting are required.

Removal of the cancerous prostate gland (radical prostatectomy) is one of the active treatment options for prostate cancer. Refinements of the techniques of

radical prostatectomy, including nerve-sparing over the last 20 years have resulted in a low perioperative morbidity and mortality and high probability of complete tumour eradication (Shipley *et al* 2006). In comparison to early prostate cancer patients undergoing watchful waiting, erectile dysfunction (45% vs. 80%) and urinary leakage (21% vs. 49%) are more common in patients treated with radical prostatectomy although the reverse applies to urinary obstruction (44% vs. 28%) (Steineck *et al* 2002). The complications of radical prostatectomy can be significantly reduced if the operation is performed in a high-volume hospital (a hospital where a high number of surgical procedures is performed) and by a surgeon who performs a high number of such procedures (Begg *et al* 2002). The risks of severe complications arising from the operative procedure, such as sepsis, myocardial infarction, rectal injury and mortality, reported from several centers of excellence are less than 1% (Shipley *et al* 2006). The advantages of radical prostatectomy as a treatment technique for early prostate cancer which include: (i) effective long-term cancer control, (ii) precise predictions of prognosis based on the pathologic features of the operative tissue specimen, (iii) pelvic lymph node dissection through the same incision and (iv) easy monitoring for detection of PSA failure of treatment to be balanced against the risks of serious operative and post-operative complications especially for patients aged 70 years or greater.

Radiation treatment either with External Beam Radiation Therapy (EBRT) or brachytherapy also provides effective long-term control for prostate cancer. During the last decade, EBRT technique has been refined as a result from development of Three-Dimensional Conformal Radiation Therapy (3D-CRT) using many high-energy photon fields individually shaped to the targeted volume and

computer software to integrate computed tomography (CT) images of the patient's internal anatomy (Shipley *et al* 2006). This advanced technique, in comparison to conventional EBRT, provides better conformality of the high dose to the shape of the tumour and reduces unwanted side effects from radiation exposure to the surrounding normal tissues. Refinement of 3D-CRT has been further achieved using intensity modulation of the radiation treatment beams (Intensity-Modulated Radiation Therapy, IMRT). IMRT has been reported to significantly increase the ratio of Tumour Control Probability (TCP) to Normal Tissue Complication Probability (NTCP) of the rectum in the treatment of prostate cancer (DeMeerleer *et al* 2000). Feasibility and safety of this highly advanced EBRT technique for localized prostate cancer has been investigated extensively. IMRT has also been reported to improve dose conformality through achievement of adequate tumour coverage and reduction of radiation exposure to normal tissues over 3D-CRT (Zelefsky *et al* 2000). EBRT can be given to patients over a wide range of ages including those with significant comorbidity (coexistence of two or more disease processes) and can also eradicate extensions of tumour beyond the margins of the prostate (Shipley *et al* 2006). EBRT may also be used to cure prostate cancer as a combined-modality treatment with hormonal manipulation therapy and brachytherapy to improve the results of treatment especially for high-risk disease. Disadvantages of using EBRT as the main treatment modality for early prostate cancer include: (i) a significant risk of sexual impotence, (ii) high (above 72 Gy) doses are required for 3D-CRT to obtain optimal treatment efficacy, (iii) a significant (~30%) risk of long-term rectal complications with increasing radiation dose and (iv) up to 50% prevalence of bladder and bowel complications during treatment persisting long-term in some patients. Not every patient can be treated

with EBRT. Contradications to treating early prostate cancer with EBRT include patients with a history of previous pelvic irradiation, active rectal inflammatory disease, very low bladder capacity, and chronic moderate or severe diarrhea from any cause.

As with EBRT, brachytherapy is a common active treatment option for localized prostate cancer. One of the techniques involves placing radioactive seeds in the prostate and around its immediate vicinity. The technology of accurate seed placement and dose distribution has been significantly improved leading to better feasibility and safety of brachytherapy as monotherapy for the effective treatment of early stage clinically organ-confined prostate cancer. Treatment outcomes and treatment-related complications after prostate brachytherapy have been improved as a result of technological improvements also reflected in measures of the quality of the implant and dose distribution. Meticulous approach, attention to detail in the operating room, close collaboration of the radiation oncologist with the medical physicist in the design of the preplan or intraoperative treatment plan, and attention to quality assurance are important contributions to a successful outcome of brachytherapy (Zelefsky & Lee 2006). Advantages of brachytherapy for early prostate cancer are cancer control rates similar to surgery and EBRT with lesser treatment times, low risk of urinary incontinence in patients without a previous history of transurethral resection of the prostate (TURP), and availability to patients over a wide range of ages including those with co-morbidities not severe enough to risk a general anesthetic. Similar to surgery and EBRT, there is a risk of sexual impotence as well as of late bowel and urinary complications although the reported risks are less with brachytherapy except for irritative bladder symptoms.

Hormone manipulation therapy has been the basis for intervention for prostate cancer as the prostate is a hormone-responsive organ (Jani and Hellman 2003). This treatment previously consisted of orchiectomy (removal of the testicles with surgery) but has been replaced by chemical castration. The broad classes of agents used to achieve this include oestrogens, progestagens, gonadotropin-releasing hormone analogues, adrenal enzyme synthesis inhibitors, and antiandrogens. There are several approaches to the administration of hormonal therapy in patients with prostate cancer, for examples, neoadjuvantly (prior to local radiation therapy), adjuvantly (administered immediately after local radiation therapy), as salvage treatment (for biochemical or clinical failure after local therapy) and as primary treatment for metastatic disease. Hormonal therapy may also be used neoadjuvantly with prostatectomy but limited success has been reported (Jani and Hellman 2003). Side effects of hormones therapy include hot flushes, loss of libido, erectile dysfunction, weight gain, gynaecomastia (breast enlargement in male due to abnormally growth of the mammary gland), liver inflammation, and osteoporosis.

Other more recent and much less widely available treatment options for localized prostate cancer include proton or heavy particles beam therapy and cryosurgery. However, some of these treatments are still considered experimental as there is no long-term data of efficacy and toxicity. Only radiation therapy techniques which are currently available at the Royal Adelaide Hospital for prostate cancer only will be further discussed in the sections which follow.

2.2 Prostate cancer radiation treatment techniques

Several radiation therapy techniques are available for treatment of prostate carcinoma at the Cancer Center, Royal Adelaide Hospital (RAH), Australia. Prior or during the period of the current work, following prostate radiation therapy techniques were available: (i) standard fractionated (2 Gy/fraction) 4-field Three-Dimensional Conformal Radiotherapy (3D-CRT) to total dose of 64 Gy, (ii) hypofractionated (2.75 Gy/fraction) 4-field 3D-CRT to total dose of 55 Gy, (iii) standard fractionated 4-field 3D-CRT to total dose of 70 Gy (4-field 3D-CRT/70 Gy) and 74 Gy (4-field 3D-CRT/74 Gy), (iv) standard fractionated 5-field 3D-CRT to total dose of 70 Gy, (v) Low-Dose-Rate Brachytherapy (LDR-BT) as monotherapy using I-125, (vi) High-Dose-Rate Brachytherapy (HDR-BT) as monotherapy using Ir-192, and (vii) combined-modality (3D-CRT and HDR-BT) treatment.

2.2.1 Three-dimensional conformal radiotherapy (3D-CRT)

Before the era of 3D-CRT, conventional radiation therapy commonly employed a four-field (box) treatment arrangement to encompass the pelvic lymph nodes, seminal vesicles, and the prostate gland. With this arrangement, the irradiated volumes were necessarily large in order to ensure full coverage of the target at risk which included subclinical and microscopic as well as gross malignant disease. The dose to the prostate, plus or minus the seminal vesicles, would then be boosted using either a similar four-field technique or rotational fields that exposed not only the disease target volumes at risk but also adjacent organs-at-risk to cumulative radiation doses in the range of 64 Gy to 70 Gy (Sandler and Michalski 2006). As the actual intended high dose disease target invariably has an irregular shape, the box-shaped or cylindrical beam arrangement of conventional radiation therapy results

in the coincidental irradiation of large amounts of bowel and bladder thus limiting the total radiation dose to 70 Gy beyond which the risks of late bowel and bladder morbidity become unacceptable (Sandler and Michalski 2006).

Advances in the development of computer technology and radiological computed tomographic scanners have made capturing of complete volumetric anatomical information possible to enable the generation of 3D radiation treatment plans and the use of customized beam apertures to shape radiation dose distributions to match the individual anatomical configuration of the intended disease target thus reducing exposure of the nearby organs-at-risk to the disease target dose. Calculation of radiation dose distributions to the organs-at-risk is also included in 3D treatment planning system. During the process of treatment planning, the dose distributions of the intended disease target and the organs-at-risk can be viewed on a 3D rendered volumetric display or in multiple reconstructions in axial, sagittal, and coronal planes. The feasibility and safety of the 3D-CRT treatment plan can be assessed using dose statistics, dose-volume histograms or predictive models of normal tissue complication probability.

Planning of a treatment with 3D-CRT involves positioning and immobilization of the patient followed by acquisition of a treatment planning CT dataset. Defining of target volumes and organs at risk is performed in the image segmentation process in which the anatomical extent of the volumes and organs are contoured on a slice-by-slice basis. Virtual simulation software tool analogous to the operational fluoroscopic isocentric radiation therapy simulator is then used to create radiation beams. The radiation beams are selected, shaped, and viewed using beam's eye view (BEV) display which allows the physicist or dosimetrist to set positions of

multileaf collimators to shape the field to encompass the projected planning target volume (PTV). Dose contributed from each beam is entered into the treatment planning software. Using a variety of dose display and analysis tools, the plan is reviewed before being finally deployed to deliver the prescription dose to the patient. Details of various 3D-CRT treatment techniques for prostate cancer available at the Cancer Center, RAH, are described in Chapter 3.

2.2.2 Brachytherapy

2001 marked the 100th anniversary of the application of brachytherapy in radiotherapy. Brachytherapy is the radiotherapy technique where the radioactive sources are placed in or near the intended target of radiation (normally tumour). The main advantage of brachytherapy is that the very short source-tumour distance allows a very high dose of radiation to be given to the tumour target whilst sparing surrounding normal tissues which receive a dose diminishing with the square of the distance from the radioactive source(s). This radiotherapy technique can be categorized in various ways. An example is by the physical relationship of the applied radioactive source to the intended target tissue; (i) the source is on the tissue surface as in a surface mold implant, (ii) the source is implanted into the tissue as in an interstitial implant, (iii) the source is in a lumen of an organ as in an intraluminal implant, and (iv) the source is in a cavity of an organ in an intracavity implant. Brachytherapy is also described according to whether the radioactive source is removed after a specified time (temporary implant) or whether it remains in the patient body forever (permanent implant). Brachytherapy is most often characterized by the dose rate of delivery of the radiation. International Committee on Radiation Units (ICRU) Report No. 38

defines Low-Dose-Rate (LDR) as 0.4 – 2 Gy/hour, Medium-Dose-Rate (MDR) as 2 – 12 Gy/hour and High-Dose-Rate (HDR) as >12 Gy/hour. Pulsed-Dose-Rate (PDR) brachytherapy which delivers the radiation dose over 1 to 3 Gy/hour does not fit into the ICRU Report No. 38 definitions but was developed to combine the convenience of high dose rate irradiation (short treatment times) with the radiobiological advantage of LDR brachytherapy.

In Australia, HDR brachytherapy with Ir-192 (remote afterloading) and LDR brachytherapy with I-125 only (permanent interstitial implant) are currently available for prostate cancer radiotherapy. The Australian Medical Service Advisory Committee for the Treatment of Prostate Cancer (2005) recommends LDR brachytherapy for patients with low risk localized prostate cancer as defined by the following criteria:

- T1 or T2 (confined within the capsule of the prostate) N0M0 disease using the TNM (Tumour, Node, Metastasis) staging system;
- Gleason scores less than or equal to 6; and
- Prostate Specific Antigen (PSA) levels less than or equal to 10 ng/ml.

HDR brachytherapy is currently used in patients with higher risk prostate cancer including locally advanced disease to supplement the radiation EBRT. The treatment efficacy and toxicity to organs-at-risk of HDR-BT as a supplement to EBRT for predominantly high risk prostate cancer have been widely reported, i.e. Limbacher *et al* (2009), Martinez *et al* (2009), Suen *et al* (2008), and Millar *et al* (2008). However, its safety and efficacy as monotherapy in low risk prostate

cancer have also been investigated (Mark *et al* 2008, Demanes *et al* 2008, Sylvester 2006, and Martin *et al* 2004).

Details of LDR-BT and HDR-BT techniques are discussed in Chapter 3.

2.3 Prostate radiotherapy complications

Complications associated with prostate radiotherapy depend on the radiation dose and irradiated volume as well as tolerance or radiosensitivity of the surrounding normal tissues. Radiotherapy toxicities may be acute (often self-limiting occurring during and up to 3 months after radiation treatment) or late (invariably irreversible occurring ≥3 months after the treatment) side-effects/complications. Acute side-effects include abdominal and pelvic symptoms such as discomfort, diarrhea, rectal bleeding and perianal soreness associated with inflammation of the rectal lining (mucosa) and urinary frequency, nocturia, dysuria, bleeding reflecting inflammation of the bladder mucosa and redness and dry flakiness of the skin, the latter being the results of mild radiation dermatitis. Acute effects usually settle completely within 2 – 4 weeks following completion of the radiotherapy (Khoo 2003) although some persist longer and may need specific treatment. The Radiation Therapy Oncology Group (RTOG) and European Organization for Research and Treatment of Cancer (EORTC) criteria for the grading of acute effects are shown in Table 2.2.

Late gastrointestinal (GI) effects (often limited to the rectum) include discharge, bleeding and stricture and late genitourinary (GU) effects such as urinary incontinence, bleeding, urethral stricture and sexual impotence are the major dose limiting complications of prostate radiotherapy. These late complications may

improve without any treatment but specific intervention ranging from simple outpatient treatment (RTOG Grade 2 effect, Table 2.3) to hospitalization and minor surgical procedures (RTOG Grade 3 effect, Table 2.3) or major surgical intervention (RTOG Grade 4 effect, Table 2.3) may be required.

***Table 2.2**. RTOG/EORTC grading criteria for acute effects (Khoo 2003)*

NOTE:
This table is included on page 23
of the print copy of the thesis held in
the University of Adelaide Library.

***Table 2.3**. RTOG/EORTC grading criteria for late effects (Khoo 2003)*

NOTE:
This table is included on page 24
of the print copy of the thesis held in
the University of Adelaide Library.

The prevalence of radiation-induced normal tissue complications following prostate radiotherapy has been reported as 6 – 19% for RTOG Grade 2 and 3 late effects and 1 – 3% for RTOG Grade 4 effects requiring major surgery (Khoo 2003). Severe RTOG Grade 4 effects are usually the results of treatments using suboptimal radiotherapy techniques such as conventional EBRT techniques, no longer in use. With more sophisticated treatment techniques such as 3D-CRT where radiation beams are individually shaped to conform to the high radiation dose target volume, exposure of the normal tissues to the high dose volume is reduced and the morbidity of radiotherapy is minimized. For example, Hanks *et al* (1995) reported reductions in rate of Grade 2 GI and GU acute toxicity in patients treated with 3D-

CRT (34%) compared with those treated with conventional EBRT (57%). Similarly men treated with conformal radiotherapy had a lower rate (37%) of late rectal bleeding and diarrhoea than those (56%) who received conventional radiotherapy for comparable efficacy of tumour control using the same dose (64 Gy in 2 Gy week-daily fractions) of radiotherapy (Dearnaley *et al* 1999).

Whilst knowledge about the effects of 3D-CRT on normal tissue toxicity was limited, the total radiation dose such as the study by Dearnaley *et al* (1999) was kept below 65 Gy in 1.8 – 2 Gy week-daily increments. A randomized radiation dose-escalation trial for the treatment of prostate cancer conducted by the M.D. Anderson Cancer Center found that although dose escalation to 78 Gy can provided better biochemical control rates, this was at the expense of a higher rate of Grade 2 or greater GI toxicity compared with 70 Gy (Kuban *et al* 2008). However, subset analysis showed that the GI complication rate in patients received 78 Gy was no greater than those receiving 70 Gy if the volume of rectum received ≥70 Gy was ≤25% (Pollack *et al* 2002). At present more sophisticated beam shaping and dose delivery techniques allow such higher total radiation doses to be easily achieved for better rates of tumour control whilst minimizing normal tissue late effects (Zietman *et al* 2005). Radiation escalated doses can not only be achieved by more sophisticated 3D-CRT such as Intensity-Modulated Radiotherapy (IMRT), but also High-Dose-Rate brachytherapy. Risk of normal tissue complications using HDR-BT for dose escalation and 3D-CRT (4-field and 5-field) but not IMRT are presented in this thesis.

Persistent radiation-induced side-effects following either LDR or HDR brachytherapy are predominantly urinary although bowel toxicity and erectile impotence may also occur (Mangar *et al* 2005). Transient side-effects of the brachytherapy procedure itself such as perineal bleeding or haematoma and mild haematuria occur commonly but these are usually mild while they last. The urinary side-effects which follow brachytherapy especially LDR are not only more persistent taking up to 9 months to settle down but are also of greater severity (Mangar *et al* 2005). They include urinary incontinence although usually only encountered in the presence of a history of transurethral resection and urethral stricture. The 5-year actuarial risk of the latter complication following LDR brachytherapy range from 5% to 12% and appears to be directly related to over-implantation of radioactive seeds into the periapical region (Merrick *et al* 2003). Late rectal complications of permanent seed implantation when they occur are usually dose and volume dependent. For example, the probability of Grade 2 late rectal morbidity was reported to be 0.4%, 1.2%, and 4.7% when the maximal rectal dose was 150, 200, and 300 Gy, respectively (Waterman & Dicker 2003). To keep the risk of late rectal morbidity at ≤5%, the doses delivered to approximately 30%, 20%, and 10% of the rectal surface are recommended not exceed 100, 150, and 200 Gy, respectively. Patients who have received LDR brachytherapy are also at risk of erectile dysfunction with a prevalence rate of around 50% at 3 years after treatment (Merrick *et al* 2005).

High-dose rate brachytherapy as monotherapy has been reported to be associated with reduced urinary and rectal toxicity as well as sexual potency rates compared with permanent seed implantation (Mangar *et al* 2005). This is supported by the

results of a Phase II trial conducted by Martinez *et al* (2001) who found that among 30 patients who received HDR-BT as monotherapy for their prostate cancer there was no instances of greater than Grade 2 RTOG acute GU and GI toxicity 4 months after treatment. Similarly, only 1 out of 43 patients treated at Osaka University Hospital with HDR-BT monotherapy for localized prostate cancer experienced RTOG Grade 4 acute toxicity and although 5 patients developed late toxicity after a median follow up of 24 months (range 1 – 76) this was mild (Yoshioka *et al* 2003). Grills *et al* (2004) reported that HDR-BT monotherapy (Ir-192) can not only achieve similar biochemical control rates as LDR (Pd-103) brachytherapy but also decreased rates of acute urinary frequency, urgency, dysuria, and rectal pain compared with LDR brachytherapy. Other groups have reported on the safety and feasibility of HDR-BT as monotherapy for localized prostate cancer, e.g. Springer *et al* 2007, Corner *et al* 2008, Demanes *et al* 2008, and Mark *et al* 2008. The expected normal tissue complications associated with HDR-BT monotherapy for patients with low risk prostate cancer will be presented in Chapter 4 of this thesis.

2.4 Second primary cancers after prostate cancer

Radiotherapy either alone or in combination with prostatectomy is an increasingly common therapeutic option for prostate cancer. However, unlike prostatectomy, radiotherapy contributes towards the development of second malignancies. The most significant information about the risk of radiation-induced cancer was derived from survivors of atomic-bomb attacks on Japan. In addition, documentation of several radiation accidents worldwide and medical reports on incidence of second cancer following radiotherapy have also provided valuable insights into this area. Hall and Wuu (2003) pointed out that the malignancies

observed in the Japanese A-bomb survivors' data were leukemias and cancers of the body lining cells (carcinomas) with no excess of sarcomas (cancers of the connective tissues including bone). The overall risk of fatal cancers was estimated to be 8% per Gy, with young children being 15 times more sensitive than middle-aged adults. In second cancers induced by radiation used to treat cancer, carcinomas were prevalent as in A-bomb survivors, especially for the normal tissues which received lower radiation doses. However, in contrast to the observations in A-bomb survivors sarcomas were reported in tissues exposed to high radiation doses. The best quantitative data or gold standard for radiation-induced carcinogenesis in humans is derived from epidemiological data obtained from Japanese A-bomb survivors which shows a clear dose-response relationship especially for the 0.1 to 2.5 Gy dose range (Figure 2.1).

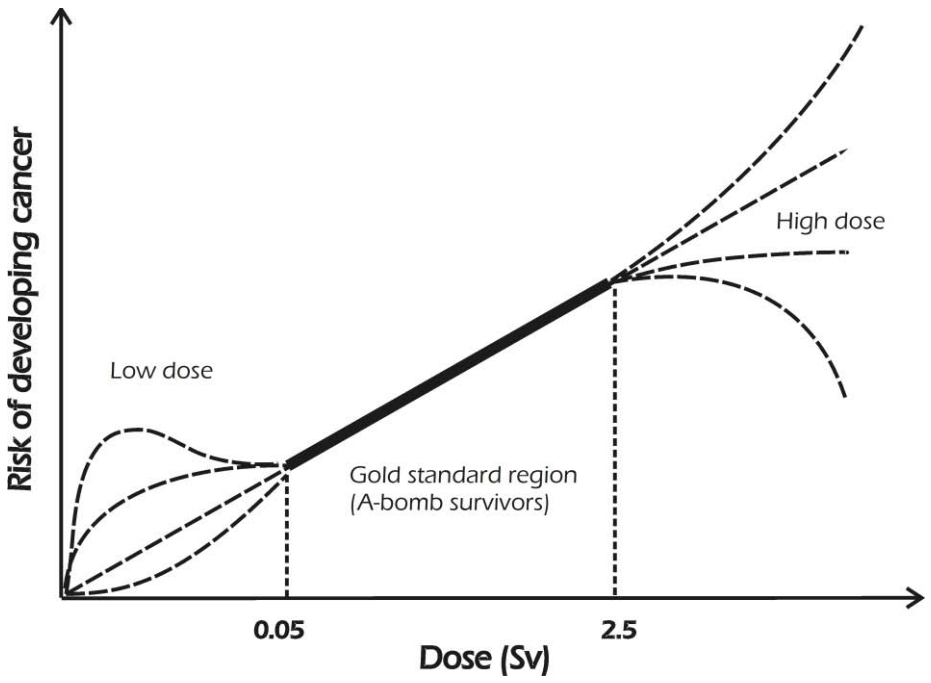

Figure 2.1*. Dose-response relationship for radiation-induced carcinogenesis in humans including the dose range with the best quantitative data and the dose ranges where there is considerable uncertainty (redrawn from figure presented in Hall 2006).*

Apart from the dose range where there is a clear dose-response relationship between radiation dose and carcinogenesis, major uncertainties exist in the relationship for the low dose and high dose regions (Figure 2.1). In prostate radiotherapy the low dose region is represented by the tissues which are located remotely from the treatment fields. These tissues receive small but significant doses (especially from external beam therapy). The high dose region is represented by the tissues which are located in the vicinity of, if not within the radiation treatment fields where moderately high doses of radiation are delivered for the tissues to survive from injury and be capable of continued proliferation. By measuring the doses which different tissues receive during prostate irradiation, the associated risks of Second Primary Cancer (SPC) can be calculated to provide information in the regions of uncertainty.

Examples of published reports on the incidence and estimated risks of secondary cancers following prostate radiation therapy are summarized in Table 2.4. Most of the data are based on epidemiologic retrospective studies (some, including more recent reports on SPC will be discussed further in Chapter 5). Other reports involve individual case studies of patients following prostate irradiation (e.g. Miller *et al* 1995, Yurdakul *et al* 2003, and Chandan & Wolsh 2003). Although a clear link between prostate cancer irradiation and the development of second malignancies in the affected normal tissues/organs is established, these case studies do not provide useful estimates of risks in the whole population of subjects whilst the retrospective studies include information about patients treated by modalities other than radiation therapy for prostate carcinoma and thus enable relative, not absolute risks of SPC to be estimated. Other limitations of these studies include

insufficient technical details to enable the risks to be correlated with the volume of normal tissues/organs irradiated with sufficient statistical confidence (Liauw *et al* 2006).

***Table 2.4**. Examples of reports on the incidence and risks of second cancers after prostate cancer radiotherapy.*

Reference	Radiotherapy Modality	No. of patients	Second cancer and status
Kleinerman *et al* (1985)	Not stated	18,135	Except for salivary gland cancer and leukemia, 15% less for all other cancers compared with general population.
Osterlind *et al* (1985)	Not stated	19,886	3% of patients developed second cancer with less than expected incidence of cancers of digestive organs and respiratory system.
Neugut *et al* (1997)	Not stated	34,889	Risk of bladder but not rectal carcinoma increased. Risk of acute non-lymphocytic or chronic lymphocytic leukemia also not increased.
Pawlish *et al* (1997)	Not stated	9,794	Around 5.5% of patients developed bladder cancer but risk increased only for patients received radiotherapy as primary treatment.
Movsas *et al* (1998)	Conformal & conventional 4-field	543	Overall, 5.7% of patients developed second cancers including lung, bladder, GI, and head and neck cancers.
Levi *et al* (1999)	Not stated	4,503	A total of 380 cases (8.4%) of second cancers reported. Incidence of lung and other tobacco-related cancers reduced.
Brenner *et al* (2000)	Not stated	51,584	6.9% of prostate patients who received radiotherapy developed second cancers of the bladder, rectum, and lung as well as sarcomas.
Gershkevitsh *et al* (1999)	Not stated	-	Non statistically significant increase in risk of leukemia.
Pickles & Phillips (2002)	Not stated	9,890	Significantly increased risks for colo-rectal cancers and sarcoma. Overall risk of second cancers 1 in 220.
Thellenberg *et al* (2003)	Not stated	135,713	Overall, second cancers found in 7.7% of patients with significantly increased risk of breast, small intestinal, renal and bladder cancers.
Abdel-Wahab *et al* (2008)	EBRT, XRT, and brachytherapy	228,235	Age-adjusted estimates of SPCs were higher with EBRT than brachytherapy and other treatments. Hazard ratio was constant with EBRT but increased with follow-up length in brachytherapy.

In addition, confounding factors such as age, race, lifestyle, and genetic predisposition in the cohorts studied make it even more difficult to separate the carcinogenic effects of prostate irradiation in the risk estimates of SPCs. A prospective study designed to minimize the influence of possible confounding factors has been suggested to estimate the real risk of second malignancy induction by prostate radiation therapy in order to confidently guide choice of treatment modality (Muller *et al* 2007). In this thesis, a radiobiological risk model is applied to the DVHs to estimate the risk of developing SPCs in the organs-at-risk without the confounding factors.

Improvements in radiotherapeutic techniques and earlier diagnosis have resulted in longer survival times for patients with treated prostate carcinoma. The longer survival times, particularly in younger patients is likely to result in increased risks of radiation-related second malignancy which will impact on decisions relating to choice of treatment (Brenner *et al* 2000). Improvements in radiotherapy techniques have inadvertently increased the possibility for the induction of potentially fatal second cancers outside of the treatment field through secondary radiations (scatter and leakage). Assessment of the risk of second malignancy in association with the out-of-field secondary radiations resulting from different radiation treatment techniques is also needed to assist in treatment choice.

Kry *et al* (2005) investigated the association between out-of-field radiation doses to normal tissues from step-and-shoot IMRT and conventional radiation treatment and the risk of second malignancies. The photon and neutron dose equivalents to 11 anatomic sites in 7 organs resulting from various treatment techniques for prostate cancer were determined using dose measurements in a Rando phantom.

Calculation of the risk of developing a fatal second malignancy was performed using the risk coefficients compiled in Report No. 116 (1993) by the National Council of Radiation Protection and Measurements (NCRP). IMRT modalities have been estimated to require 3.5 – 4.9 times as many monitor units to deliver dose fraction compared to conventional 3D-CRT. The absolute risk of inducing second cancer was therefore found to be the lowest (1.7%) for the conventional 3D-CRT because the number of Monitor Units (MU) required for this treatment approach was the lowest. The IMRT treatment with the lowest absolute risk was that from 10 MV photon Varian accelerator (2.1%), even lower than that for the 6 MV photon machine because fewer MUs were required for treatment using the 10 MV accelerator. The risks from the 15 MV Varian and Siemens accelerators using IMRT were 3.4% and 4.0% respectively, because of the increased neutron production by treatment machines at this higher energy level. The 18 MV IMRT modality was therefore found to be associated with the largest absolute risk of fatal second malignancy of 5.1% because of the greatest neutron dose contribution. Comparison of the Siemens and Varian accelerators showed that the Siemens accelerator produced larger total dose equivalents for the same energy level resulting in a greater calculated risk of fatal second malignancy. Higher out-of-field dose equivalents therefore result in higher risks for IMRT treatments compared with conventional 3D-CRT. However, substantial variability in these risks for different IMRT treatments was observed in this investigation which attempted to determine and compare the association between out-of-field dose equivalents and the risk of developing potentially fatal second cancers from two different treatment techniques, step-and-shoot IMRT and conventional 3D-CRT.

In this thesis, a radiation dosimetry technique based on thermoluminescence dosimeters is established to measure out-of-field and peripheral radiation doses in order to estimate the risk of developing SPC in organs/tissues not within the therapeutic radiation field for localized prostate cancer. With these measurements and the use of the radiobiological risk model discussed in Chapter 5 to analyze the dose-volume histograms, it is possible to estimate the risk of radiation-induced SPCs in organs/tissues within the prostate radiation field as well as organs/tissues located distant from the target of treatment exposed only to secondary radiations produced from interactions of the primary radiation beams.

2.5 Conclusion

Localized prostate cancer can be managed by prostatectomy, radiation therapy, or close observation. Each management approach has its advantages and disadvantages. Following prostate cancer radiation treatment, a small (≤5%) risk of normal tissue complications is accepted as a trade of for control of the cancer. The level of risk of normal tissue complications depends on the dose received, treatment technique, and radiobiological response characteristics of normal tissue. Although most of the late radiation effects are low grade and do not require hospitalization or major surgical intervention for management, some are potentially life threatening and require vigorous in-patient treatment. It is now also acknowledged that prostate cancer radiotherapy is associated with an increase in the risk of development of second malignancies compared to patients treated with surgery. This risk is enhanced for prostate cancer patients because of earlier diagnosis and longer survivorship. Assessment of NTCP and risk of second malignancy following radiation treatment for prostate cancer is urgently needed

because the increasing number of patients now diagnosed are faced with a wide choice of radiation treatment modalities such as 3D-CRT, IMRT, LDR-BT and HDR-BT either alone or in combination. The risk estimates are important in treatment decision making particularly for low risk prostate cancer where the risk of developing a treatment related complication may exceed the risk of dying of prostate cancer.

Chapter 3

Normal Tissue Complication Probability

3.1 Introduction

Volumetric control of the dose distribution in radiation treatment planning is currently determined through a multi-factorial, quantitative decision making process (Luxton *et al* 2008). The treatment plan is optimized by using physical approaches to maximize dose to the tumour target and also to minimize doses to surrounding critical normal tissue structures. The latter strategy is very important because critical normal structures or Organs-At-Risk (OARs) are often partially irradiated to the same high therapeutic doses of radiation as the tumour target which has the potential to increase treatment-related complications. Tumour Control Probability (TCP) and Normal Tissue Complication Probability (NTCP)

statistical models which relate treatment and clinical factors to the probability of the respective treatment outcomes may be employed to evaluate the treatment plan. In this chapter, the basis of NTCP models only is addressed.

Modern knowledge of normal tissue tolerance is based on a seminal publication by Emami *et al* (1991). Values of tolerance based on uniform irradiation of 28 critical normal tissue structures and complication rates reported in the clinical literature were compiled. In the same year Burman *et al* (1991) published tolerance dose data based on a phenomenological NTCP model proposed by Lyman in 1985 and proposed this as the basis of NTCP determination. Soon after this, several algorithms were proposed to convert a heterogeneous dose-distribution into a uniform dose-distribution, this facilitating the use of Lyman's model in clinical radiotherapy where dose distributions in the tumour target volume as well as OARs are often heterogeneous. In the following sections, Lyman's NTCP model and associated algorithms as well as several other models used in prediction of normal tissue complications such as the relative seriality model, the critical volume model, the parallel architecture model, and the cluster model will be presented.

3.2 NTCP models

3.2.1 Lyman model

Lyman NTCP model is based on an error function with 4 parameters which connects three variables of interest; normal tissue complication probability, dose (D) and partial volume (v). The interrelation of the variables can be described by the following equation (Burman *et al* 1991):

$$NTCP = \frac{1}{\sqrt{2\pi}} \int_{-\infty}^{t} exp\left(\frac{-t^2}{2}\right) dt\,, \tag{3.1}$$

where,
$$t = \frac{\left(D - TD_{50}(v)\right)}{m * TD_{50}(v)}, \tag{3.2}$$

with,
$$v = \frac{V}{V_{ref}}, \tag{3.3}$$

and,
$$TD(v) = TD(1) * v^{-n}. \tag{3.4}$$

TD is the tolerance dose and v is the fraction of an irradiated organ or the volume relative to some reference volume. TD_{50} is the dose to the whole volume (or reference volume) which would result in 50 percent probability of a complication. Parameter n (range from 0 to 1) defines the volume dependence of the complication probability while parameter m represents the slope of the curve relating complication probability to dose. V_{ref} is the reference volume for TD_{50}. $TD_{50}(1)$ is the tolerance dose for uniform irradiation of the entire organ.

Most of the model parameters described above have been derived from the report of Emami *et al* (1991). The value of model parameters for specific radiation-induced end points in several organs are tabulated here (Table 3.1).

The tolerance dose (in Gy) of a particular organ may also be defined as $TD_{5/5}$ (the 5% probability of a complication within 5 years after treatment) or $TD_{50/5}$ (the 50% probability of a complication within 5 years after treatment). However, only $TD_{50/5}$ is used in the calculation of NTCP for the current work in this thesis.

Table 3.1. *End points of normal tissues and model parameters (Burman et al 1991)*

Organ	Model parameters				End-points
	V_{ref}	n	m	TD_{50} (Gy)	
Bladder	Whole organ	0.5	0.11	80	Symptomatic bladder contracture and volume loss
Colon	Whole organ	0.17	0.11	55	Obstruction/perforation/ ulceration/fistula
Femoral head & neck	Whole organ	0.25	0.12	65	Necrosis
Lung	Whole organ	0.87	0.18	24.5	Pneumonitis
Rectum	Whole organ	0.12	0.15	80	Severe proctitis/necrosis/ stenosis/fistula
Small intestine	Whole organ	0.15	0.16	55	Obstruction/perforation
Spinal cord	20 cm	0.05	0.18	66.5	Myelitis/necrosis

From Table 3.1, it can be seen that the NTCP of lung has high volume dependency as reflected in the high value (0.87) of the parameter *n*. Radiation pneumonitis, therefore, results when a large volume of lung tissue is irradiated to a relatively low dose, hence the low TD_{50} of lung compared with other organs. In contrast, despite the relatively high TD_{50} (66.5 Gy) irradiation of small fractions of spinal cord which this shows low volume dependency (n = 0.05) results in radiation myelitis/necrosis. The Lyman model, therefore, demonstrates the strong association between (tolerance) dose and irradiated volume in the prediction of normal tissue complication probability.

When an entire normal organ receives a single homogeneous dose of radiation, its NTCP can accurately predicted using equation 3.1, 3.2, 3.3, and 3.4 above. However, as previously implied the Lyman model for NTCP determination is based on uniform irradiation of OARs but this situation seldom applies in clinical radiotherapy. In clinical practice usually involving delivery of External Beam Radiation Therapy (EBRT), each OAR receives a range of doses of ionizing radiation. Information on the dose-volume distribution is therefore required to adequately evaluate a treatment plan. A Dose-Volume Histogram (DVH) which represents the relationship between dose and irradiated volume of the organ/tissue at risk is an important tool in the estimation of NTCP. There are two types of DVHs, differential and cumulative DVH. Differential DVH (Figure 3.1) is a plot of the frequency of volumes on the y axis receiving a range of specified doses defined in ascending equi-spaced dose intervals on the x axis while cumulative DVH (Figure 3.2) is a plot of volume on the y axis receiving a dose greater than or equal to the dose level defined by ascending dose intervals on the x axis (Kutcher & Burman 1989). Evaluation of a treatment plan by NTCP using DVH data directly is problematic because of the copious dose-volume distribution information in the DVH. Hence, transformation of DVH is required in order to obtain representative data based on a single dose-volume pair, i.e. effective dose-whole volume or effective volume-maximum dose (see following sections for details) which can be used in the model.

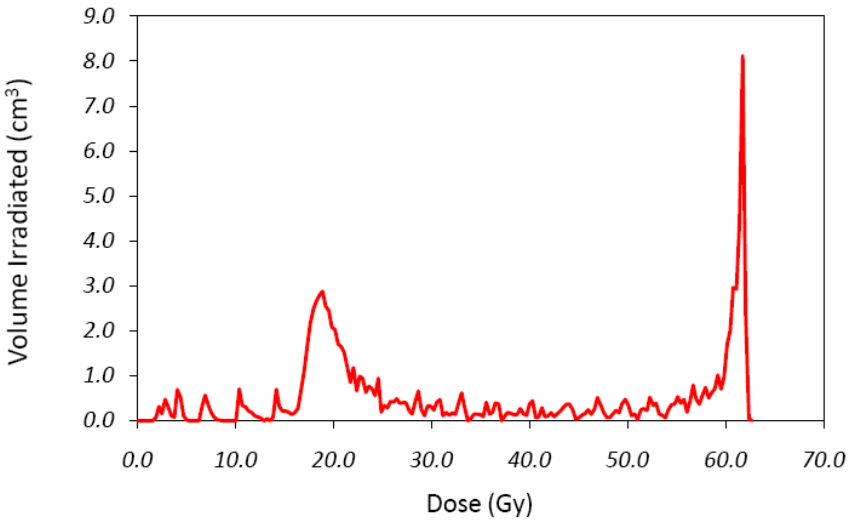

Figure 3.1. *An example of differential DVH derived from irradiation of rectum from standard 4-field 3D-conformal radiotherapy (3D-CRT) for prostate cancer.*

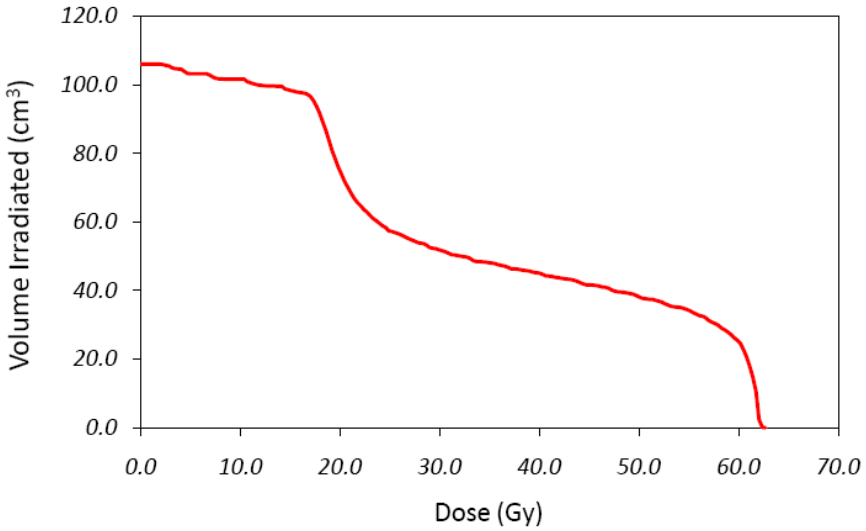

Figure 3.2. *An example of cumulative DVH derived from irradiation of rectum from standard 4-field 3D-conformal radiotherapy (3D-CRT) for prostate cancer.*

3.2.1.1 Lyman and Wolbarst DVH reduction scheme

Lyman and Wolbarst (1987) proposed an approach by which a DVH for an OAR irradiated to non-uniform dose can be reduced to a uniform histogram by using an interpolation scheme. In this approach, a special function defined as *C(D,V)* represents the probability that under a specified time-fractionation schedule, a well-defined biological end-point will occur if a fraction *V* of the OAR is irradiated uniformly to dose level *D* while the remainder of OAR (1 – *V*) receives zero or negligible dose (Figure 3.3).

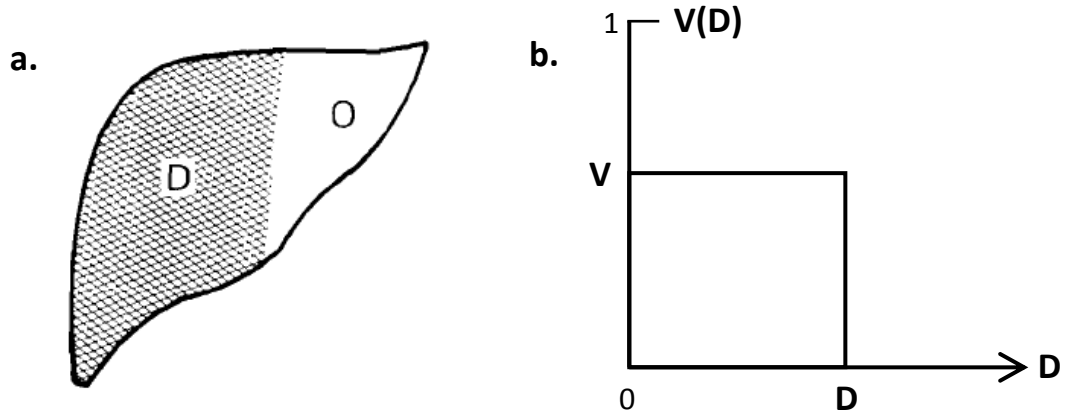

Figure 3.3. *The experimental situation corresponding to one point on the C(D,V) surface for some particular fixed regimen of time, dose, fractionation, RBE, etc. (a) The fraction V of the organ receives dose D, and the rest receives none. (b) The corresponding dose-volume histogram (Lyman and Wolbarst 1987).*

Determination of the likelihood of complications arising when dose is non-uniformly distributed throughout the whole organ is described by a multi-step DVH (Figure 3.4) and carried out following transformation of the multi-step DVH into an equivalent single-step DVH.

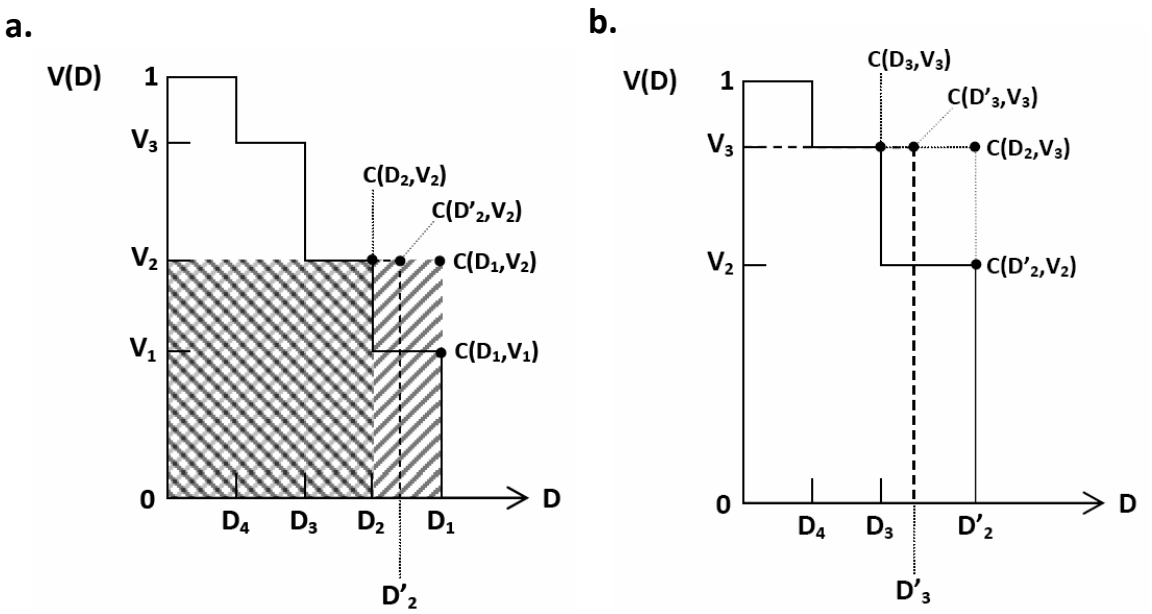

Figure 3.4. *Graphic illustration of multi-step dose-volume histogram and the first two steps of the histogram-reduction process as proposed by Lyman and Wolbarst (1987).*

The process of histogram-reduction as described by Lyman and Wolbarst (1987) includes several stages. In the first stage, the two highest-dose steps (D_1,V_1 and D_2,V_2) are replaced with a single step (D'_2,V_2) showed as the dashed line (Figure 3.4a) which represents the volume V_2 taken to the intermediate dose D'_2 to maintain volume normalization. It is assumed that replacing the first two highest-dose steps by an intermediate dose D'_2 has no effect on the radio-responsiveness of the lower-dose regions and coalescence of the two remaining highest dose steps into one has little effect on the results of subsequent stages of the calculation.

Various approaches can be used to estimate the D'_2. Firstly, the estimation of D'_2 value can be based on a volume-weighted averaging of D_1 and D_2 steps (Figure 3.4a):

$$D'_2 = D_2 + (V_1 / V_2) * (D_1 - D_2). \qquad (3.5)$$

However, non-linearities of C(D,V) in D and V are not adequately handled by this approach.

Another approach can be used to calculate D'_2 value. From equation (3.5) it can be seen that if value of V_1 gets smaller ($V_1 \rightarrow 0$), the magnitude of $C(D'_2,V_2)$ shifts toward $C(D_2,V_2)$. In contrast, as the value of V_1 gets close to that of V_2, the magnitude of $C(D'_2,V_2)$ approximates to $C(D_1,V_2)$. Accordingly, $C(D'_2,V_2)$ may be expressed as a linear combination of $C(D_1,V_2)$ and $C(D_2,V_2)$ weighted by proportion to their respective volume:

$$C\left(D'_2,V_2\right)=\left[\left(V_2-V_1\right)/V_2\right]*C\left(D_2,V_2\right)+\left(\frac{V_1}{V_2}\right)*C\left(D_1,V_2\right). \qquad (3.6)$$

This approach can be seen to be valid in the approximation of $C(D'_2,V_2)$ if sufficiently small steps in V and D are used.

The next stage of histogram reduction is using a similar process as in the first stage by replacing the remaining two highest-dose steps (D'_2,V_2 and D_3,V_3) with the intermediate dose step (D'_3,V_3) as shown in figure 3.4b and the following equations:

$$C\left(D'_3,V_3\right)=\left[\left(V_3-V_2\right)/V_3\right]*C\left(D_3,V_3\right)+\left(\frac{V_2}{V_3}\right)*C\left(D'_2,V_3\right). \qquad (3.7)$$

And for any *i* greater than 1,

$$C\left(D'_{i+1},V_{i+1}\right)=\left[\left(V_{i+1}-V_i\right)/V_{i+1}\right]*C\left(D_{i+1},V_{i+1}\right)+\left(\frac{V_i}{V_{i+1}}\right)*C\left(D'_i,V_{i+1}\right). \qquad (3.8)$$

The process as described above can be repeated until after N – 1 iterations for N-step patient histogram, the final single-step histogram with a corner at $(D'_N,1)$ is

eventually obtained. This final single step-histogram can be used to estimate the probability of the complication in the critical organ defined as C(D,V) with the given dose distribution. The probit or integrated standard normal function can be used to obtain the complication probability as follows:

$$C(D,V) = C(t) = (2\pi)^{-1/2} \int_{-\infty}^{\infty} exp\left(-\frac{t^2}{2}\right) dt', \qquad (3.9)$$

where, $$t = \lfloor D - TD_{50/5}(V) \rfloor / \sigma(V). \qquad (3.10)$$

The normal deviate *t* is defined as the number of standard deviations by which the point (D,V) is away from $TD_{50/5}$(V), and:

$$TD_{50/5}(V) = TD_{50/5}(1)/V^n. \qquad (3.11)$$

The expression σ(V) in equation (3.10) is defined as:

$$\sigma(V) = m * TD_{50/5}(V). \qquad (3.12)$$

It can be seen that complication probability C(D,V) obtained with this approach is fully parameterized by $TD_{50/5}(1)$ which is the tolerance dose for uniform irradiation of the entire organ, the exponent *n* (volume effect), and the coefficient *m* (dose-response relationship).

3.2.1.2 Kutcher and Burman DVH reduction scheme (Effective Volume)

The DVH reduction scheme called the effective volume method was developed by Kutcher and Burman (1989). This method transforms an original non-uniform cumulative dose-volume histogram (figure 3.5) to a uniform one which contains an effective volume (V_{eff}) and a dose equal to the maximum dose (D_m) to the organ.

This transformed histogram is assumed to introduce the same complication probability as the original one. The complication probability may be calculated using a known complication probability model for uniform partial organ irradiation.

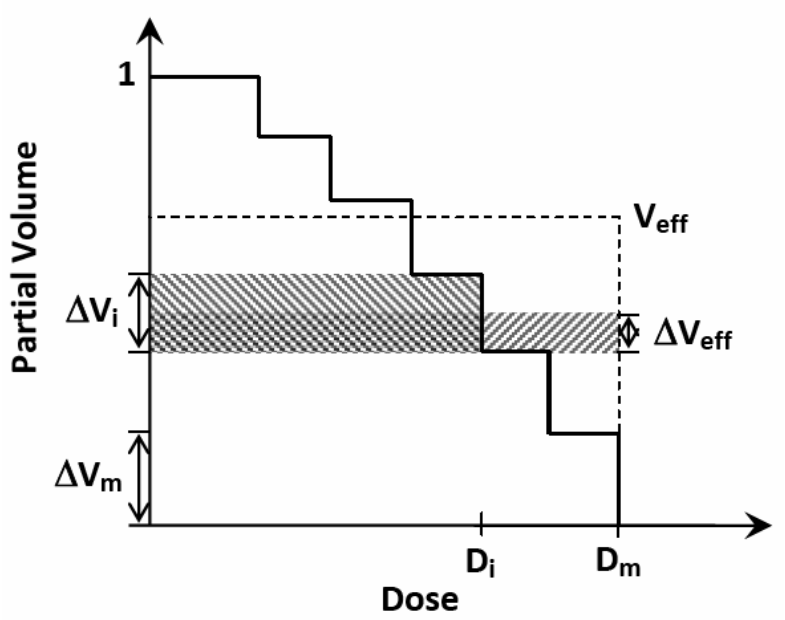

Figure 3.5. *Step function representation of a dose volume histogram (Kutcher & Burman 1989).*

Each step of a histogram represented by volume ΔV_i and dose D_i in Figure 3.5 is assumed to comply with a power law relationship so an effective volume $\Delta\left(V_{eff}\right)_i$ for this step may be calculated using following equation:

$$\left(\Delta V_{eff}\right)_i = \Delta V_i \left(\frac{D_i}{D_{max}}\right)^{1/n}, \qquad (3.13)$$

where *n* is a size (volume effect) parameter.

This process is repeated to every step of a cumulative DVH so that the effective volume for the entire DVH is given by:

$$V_{eff} = \frac{1}{V_{ref}} \sum_i \Delta V_i \left(\frac{\Delta D_i}{D_{max}} \right)^{1/n}, \qquad (3.14)$$

where V_{ref} is an entire volume of an organ or a reference volume.

The most important assumptions made for this DVH reduction method is that a power law relationship for tolerance dose holds for uniform irradiation of the organ and that this rule can be applied independently to each volume element of the histogram (Kutcher and Burman 1989). Therefore, the adjustments made independently for each volume element can be combined to produce the effective volume as given in equation (3.14).

When the process of DVH reduction is completed, NTCP can be calculated with the Lyman model using equation (3.1) and the equations following that as defined below:

$$NTCP = \frac{1}{\sqrt{2\pi}} \int_{-\infty}^{t} exp\left(-\frac{t^2}{2} \right) dt, \qquad (3.1)$$

where,
$$t = \frac{D_{max} - TD_{50}\left(V_{eff}\right)}{m * TD_{50}\left(V_{eff}\right)}, \qquad (3.15)$$

and,
$$TD_{50}\left(V_{eff}\right) = TD_{50}\left(1\right) * V_{eff}{}^{-n}. \qquad (3.16)$$

The NTCP model as proposed by Lyman and the accompanying Lyman and Wolbarst or Kutcher and Burman DVH reduction schemes have been widely used to estimate the probability of complications in OAR's which arise as a result of radiation treatment. The normal tissue tolerance data and parameters presented in Emami *et al* (1991) and Burman *et al* (1991) have been and are still used extensively for such purposes although many researchers have reported new

model parameters for several normal tissues. Despite the availability of new model parameters, Emami and Burman tolerance data and parameters are nearly always used because new estimates are usually derived from data collected at a single institution and may not be applicable to other patient populations (Semenenko and Li 2008). Toxicity data from various institutions have been collected and analyzed to fit to new NTCP models such as the attempts of Kwa *et al* 1998 and Rancati *et al* 2007. However, parameters obtained from these attempts still need to be validated before they are able to be widely applied in clinical practice.

In conjunction with normal tissues tolerance data of Emami *et al* (1991) and Burman *et al* (1991), the Lyman NTCP model has become the most popular empirical model for NTCP calculation. This is because of the readily availability of tolerance data for most of normal organs/tissues at risk for radiation-induced end points of interest in the clinical setting to enable NTCP calculations using the model. However, the Lyman model cannot directly handle the non-uniformity of treatment dose distributions and converting or reducing the DVH into an equivalent uniform dose distribution which is a major disadvantage of the model. Although the study of Cozzi *et al* (2000) showed that DVHs converted or reduced differently produced similar results for quasi-uniform dose distributions, very different results were generated in real clinical situations where large-dose inhomogeneities in the organ/tissue occur. Therefore, the risk of getting opposite ranking of the same dose plans analyzed with different DVHs reduction schemes is high thus limiting of the use of the Lyman model in the empirical evaluation radiation treatment plans.

3.2.2 Relative Seriality (RS) model

Kallman *et al* (1992) proposed the Poisson model of cell survival to evaluate non-uniform irradiation of OARs from fractionated radiotherapy. A new parameter called the "relative seriality" or "*s*" parameter is used to take into account the complex structural and functional organization of OARs as well as of tumour tissues. In Kallman's model, the volumetric response of an organ or tissue to irradiation depends on whether its structural and functional organization is that of a parallel or serial organ/tissue. A parallel organ is characterized by a small value of "*s*" parameter (close to zero) and exhibits strong volume dependence in its response to irradiation. In contrast, the value of "*s*" parameter of a serial organ/tissue is close to unity and exhibits a weak dependency in its volumetric response to irradiation. However, no organ/tissue is purely serial or parallel although studies suggest that the majority of organs/tissues are preferentially parallel (Kallman *et al* 1992), as reflected in value of the relative seriality parameter for a variety of organs/tissues illustrated in Table 3.2

Table 3.2. *Radiobiological data corresponding to relative seriality model (Kallman et al 1992).* D_{50} *in this table approximates the* $TD_{50}/5$ *years.*

NOTE:
This table is included on page 49
of the print copy of the thesis held in
the University of Adelaide Library.

For some organs/tissues, the value of "*s*" parameter is larger than unity such as bladder and esophagus (Table 3.2). Such organs /tissues have very weak volume dependence in their response to irradiation. The values of "*s*" parameter were obtained by fitting clinical data to the model and vary according to the clinical study from which the data were derived. Inconsistencies of the model may also be related to the relative seriality model being based more on phenomenological (mathematically expressed values derived from clinical observations) than radiobiological considerations (Stavreva & Stavrev 2002).

As discussed above, there is no organ/tissue which is purely parallel (Figure 3.6a) or serial (Figure 3.6b) in its structural and functional organization but rather there is a mix of both types. This mix of both serial and parallel types (Figure 3.6c) is a more realistic representation of the organization of any organ/tissue. The properties of such as organ/tissue are controlled by parallel (*n*) and serial (*m*) structural parameters as well as by parallel (*a*) and serial (*b*) fractions of the organ/tissue (see Figure 3.6c).

If P is a response function for a uniformly irradiated tissue, the response function P_v of a subunit v of a tissue can then be determined using the following equation (Kallman *et al* 1992):

$$P_v = \left(1 - \left(1 - P^s\right)^v\right)^{1/s}. \qquad (3.17)$$

Equation (3.17) may be inverted and written in terms of P assuming a homogeneous dose distribution to all functional subunits with survival P_v at dose D (Kallman *et al* 1992):

$$P = \left(1 - \left(1 - P_v^s\right)^{1/v}\right)^{1/s}. \qquad (3.18)$$

NOTE:
This figure is included on page 51 of the print copy of the thesis held in the University of Adelaide Library.

Figure 3.6. *A schematic illustration of a serial-parallel structure (Kallman et al 1992). Figure 3.6a illustrates the organ with pure parallel (m) structure; Figure 3.6b shows the functional organization of a serial (n) organ and Figure 3.6c represents an organ with parallel as well as serial functional subunits.*

In the situation of non-uniform dose distribution when the entire organ with homogeneous density is irradiated, its response can be expressed as (Kallman *et al* 1992):

$$P = \left[1 - \prod_{i=1}^{M}\left[1 - \left(P_{\Delta V}\left(D_i\right)\right)^s\right]\right]^{1/s}, \qquad (3.19)$$

where ΔV is the fractional volume of a volume element or voxel which is equal to the reciprocal of the number of voxels M of the whole organ.

The $P_{\Delta V}(D_i)$ term in equation (3.19) may be written in terms of P for the whole organ using equation (3.17) which becomes:

$$P = \left[1 - \prod_{i=1}^{M} \left[1 - P\left(D_i\right)^s \right]^{\Delta V} \right]^{1/s}. \qquad (3.20)$$

The response of the entire organ P to non-uniform dose distribution is now described as a function of the response of the whole organ for the D_i in each compartment i (Kallman *et al* 1992).

The relative seriality model may be written in form of logistic type model as described in MacKay *et al* (1997):

$$P\left(D_i\right) = \left[1 + \left(\frac{D_{50}}{D_i} \right)^k \right]^{-1}, \qquad (3.21)$$

where $P(D_i)$ is the probability of complication for an organ irradiated to dose D_i, D_{50} is the dose that contributes to 50% complication following whole organ irradiation and the slope of the dose-response curve where $D = D_{50}$ is $k/4D_{50}$. The value of parameter k can be deduced from the 5% (D_{05}) and 50% (D_{50}) tolerance doses using the following equation:

$$k = \frac{ln19}{ln\left(D_{50}/D_{05}\right)}. \qquad (3.22)$$

Alternatively, the value of parameter k may be calculated from the following formalism as proposed by Niemierko & Goitein (1993):

$$k = \frac{4}{\sqrt{2\pi} * m}, \tag{3.23}$$

where, *m* the parameter in Lyman's NTCP model represents the steepness of the dose-response curve.

Replacing $P(D_i)$ term in equation (3.20) with equation (3.21), the relative seriality NTCP model can now be written as follows:

$$NTCP = \left[1 - \prod_{i=1}^{M} \left[1 - \left(\frac{1}{1 + \left(D_{50} / D_i \right)^k} \right)^s \right]^{\Delta V} \right]^{1/s}. \tag{3.24}$$

The equation (3.24) is then used to determine the probability of complication following inhomogeneous irradiation of an organ/tissue.

The main difference between the Lyman (based on probit function), and the two relative seriality (one based on logistic and the other based on Poisson functions) models is that the models based on probit and logistic functions are mathematically easier to use when analysing a large amount of clinical data but are less credible as they have no biological bases although the calculated probability of complications approximate the expected sigmoidal curve dose relationship (Kallman *et al* 1992).

3.2.3 Other NTCP models

Several other NTCP models have been developed for evaluation of a radiation treatment plan. For example, the critical element model (Schultheiss *et al* 1983 and Niemierko & Goitein 1991) is based on the concept that the organ/tissue consists of numerous functional subunits (FSU) defining its structural or functional

organizations and that the organ/tissues can be divided into three fundamentally different radiation response categories (Withers *et al* 1988 and Niemierko & Goitein 1991): (a) Critical response (e.g. spinal cord, nerves, peritoneum) – the organ/tissue is composed of many FSUs but damaging of any single FSU will result in a complication affecting the entire structure; (b) Integral response (e.g. kidney, liver, lung) – a complication results if a substantial number of FSUs of the constituent organ/tissue are damaged and (c) Graded response (e.g. skin, mucosa) – the severity of the complication occurs on a continuous scale which escalates with the number of damaged FSUs.

Therefore, few assumptions are made in the critical element model: other than (i) each organ/tissue consists of a number of identical elements or FSUs, (ii) each element or FSU responds to radiation independently and (iii) the complication is expressed when one or more elements are damaged and although the severity of radiation damage is variable each element of an organ/tissue is considered critical in the expression.

The parallel architecture model was reported by Jackson *et al* (1993), Yorke *et al* (1993), and Niemierko & Goitein (1993). This model is also based on the concept of the organ/tissue being composed of a number of functional subunits but the model only applies to those organs/tissues with parallel architecture such as lung and kidney. A parallel organ/tissue composes of subunits which are organized to function independently so that a complication results only if a critically large number of FSUs is damaged by radiation. Hence, the normal tissue complication probability is determined by the number or fraction of functional subunits of an organ/tissue which survives after irradiation. It has been suggested that individual

variations in organ/tissue radiosensitivity as well as that for the whole patient population are taken into account in this model. Furthermore, although the model was developed for parallel organs/tissues which demonstrate an integral response defined by the critical element model, it has been suggested that the parallel architecture model can be applied to serial organs/tissues which show a critical response in the critical element model such as spinal cord etc.

According to the concepts underpinning the two NTCP models above, the probability of complication arising in an organ/tissue is related to depletion of the functional subunit organization of the organ/tissue specifically the number of FSUs affected depending on whether the organ/tissue is organized to function serially or in parallel. However, Thames *et al* (2004) suggested that the probability of complication of OARs is also determined by the spatial location of the damage FSUs. A new NTCP model called "cluster models" based on this suggestion has been proposed. The new model assumes that the density of damaged FSUs in an organ/tissue increases with increasing radiation dose but that the probability of a complication arising is determined by the spatial distribution of the damaged FSUs as well as the absolute numbers of damaged FSUs. Hence, a complication arises in the organ/tissue when sufficiently large aggregates (cluster) of sterilized FSUs have accumulated in the vicinity of the delivered radiation dose. With this model, it has been noted that variations in distribution of "hot spots" in treatment plans with identical dose-volume histograms will lead to variability in the complication probability. However, current description of cluster models is limited to one and two dimensions and based on homogeneously irradiated organs/tissues. Further studies carried out by authors including analysis of DVH data taking into account

the wide variability in the distribution of hot spots as well as inhomogeneity of dose distributions in these dimensions should help in the further development of the cluster model.

In this chapter various NTCP models have been presented to assist in the evaluation of radiation treatment plans. Ideally, a set of parameters which fits well with the clinical data should be applied to minimize uncertainties of modelling results. Primarily, the selection of an appropriate model to examine the dose-volume data in this thesis is based on the ability of the model to take into account the dose-distribution inhomogeneities as well as biophysical properties (such as structural architecture of functional subunits) in the NTCP calculations. The relative seriality model is preferentially used in the most of evaluations of the treatment plans in this thesis for such reasons. However, the femoral heads are assessed by the Lyman model because the parameters for the relative seriality model are not available for evaluation of this structure using. A set of widely used parameters reported in the literature have been utilized and the variation of NTCP as a function of these parameters has also been investigated in this thesis.

3.3 Physical dose conversion

The doses in the original dose-volume histograms in this thesis are physical doses absorbed by actual normal tissues which constitute the organs-at-risk. These doses are not meaningful when evaluating biological response corresponding to the different radiation treatment modalities. To address this, radiobiological parameters are applied to convert physical doses to doses with biologically meaningful end points. In addition, it is well acknowledged that late effects are

highly sensitive to changes in fractionation (Hall 2000) which means that different radiation dose schedules delivered by the various radiation treatment techniques vary in biological effects such as NTCP. Therefore, physical dose in all original dose-volume histograms in this thesis are normalized to specified biological end-points and to the same standard radiation dose schedule (2 Gy/fraction) using two successive physical dose conversion processes.

3.3.1 Biologically Effective Dose and Relative Effectiveness

Biologically Effective Dose ($BE_{ff}D$) or Extrapolated Response Dose (ERD) as originally suggested by Barendsen (1982) and later renamed $BE_{ff}D$ (Jones *et al* 2001) is based on the linear quadratic (LQ) model of radiation effect. Radiation cell kill (or effect, *E*) may be expressed as:

$$Cell\ Kill = E = n*\left(\alpha d + \beta d^2\right), \qquad (3.25)$$

where α and β are the radiosensitivity coefficients, *n* the number of fractions and *d* the dose per fraction which makes the total dose (*D*) = *nd*.

If the dose per fraction (*d*) is progressively reduced until a value of zero is approached, the number of fractions (*n*) needs to be increased to maintain the same effect. Accordingly, the value of βd^2 will be very small in comparison to αd (as value of *d* will be much larger than d^2 for very small value of *d* and α is always larger than β). Hence, with very small value of *d*, equation (3.25) can be written as:

$$E = n\alpha d = \alpha D. \qquad (3.26)$$

It can be demonstrated from the above relationships that to achieve a specific radiation effect, a very large total dose (*D*) must be given with a very small dose

per fraction. The total dose required in these conditions constitutes the definition of $BE_{ff}D$ in situations where cellular repopulation can be ignored, therefore, in this limiting case (Jones *et al* 2001):

$$BE_{ff}D = D = \frac{E}{\alpha}. \qquad (3.27)$$

Therefore, $BE_{ff}D$ represents the physical dose required for a given effect if the dose is to be delivered by infinitely small doses per fraction or, in the case of continuous irradiation, at a very low dose rate.

For the case of any practical radiotherapy schedule, $BE_{ff}D$ can be calculated by dividing both sides of equation (3.25) by α to obtain:

$$BE_{ff}D = \frac{E}{\alpha} = \frac{n\left(\alpha d + \beta d^2\right)}{\alpha} = nd\left[1 + \frac{d}{\left(\alpha/\beta\right)}\right], \qquad (3.28)$$

then,
$$BE_{ff}D = D\left[1 + \frac{d}{\left(\alpha/\beta\right)}\right]. \qquad (3.29)$$

The terms in the bracket in equation (3.29) is called Relative Effectiveness (RE) per unit dose so the general term of $BE_{ff}D$ may be written as:

Biological Dose ($BE_{ff}D$) = Total Physical Dose x *RE*. (3.30)

Dale (1985) demonstrated the use of the above equations to obtain relative effectiveness for various fractionation schedules. In its general form, RE can be written as:

$$RE = 1 + D\left(\frac{\beta}{\alpha}\right). \qquad (3.31)$$

For fractionated treatments delivering n individual dose of magnitude d_n with space between fractions sufficiently long enough to allow full recovery of sub-lethal damage, the effect of such irradiation may be written as (Dale 1985):

$$E = n\left(\alpha d_n + \beta d_n^2\right), \tag{3.32}$$

and,

$$\frac{E}{\alpha} = nd_n\left[1 + d_n\left(\frac{\beta}{\alpha}\right)\right]. \tag{3.33}$$

Because nd_n is the total dose administered and the left hand side of the above equation depends only on the chosen level of effect, RE for fractionated radiotherapy, hence, may be expressed as suggested by Dale (1985):

$$\left(RE\right)_{fractionated} = 1 + d_n\left(\frac{\beta}{\alpha}\right). \tag{3.34}$$

From equation (3.30), it is evident that the total dose (D) required in any radiation treatment regime is related to $BE_{ff}D$ and RE as:

$$Total\ Dose\ (D) = BE_{ff}D/RE \tag{3.35}$$

Dale (1985) described radiation damage as being of Type A and Type B. Type A damage may be described as damage which occurs as a result of simultaneous hits on each of the two critical targets in one radiation event whilst Type B damage occurs due to a lethal combination of the damage inflicted on each target in two separate radiation events. Total Type A damage is represented by αD and total Type B damage by βD^2. Then, average relative effectiveness per unit dose is defined as:

$$RE = 1 + \frac{Total\ Type\ B\ Damage}{Total\ Type\ A\ Damage}. \tag{3.36}$$

Thus, for acute irradiation,

$$RE = 1 + \frac{\beta D^2}{\alpha D}, \tag{3.37}$$

which is equivalent to equation (3.31).

For protracted (continuous) irradiation at constant dose rate (no decay of radiation source), a small probability (p) per unit dose that sub-lethal damage occurs following irradiation at dose rate R in time dt is (Dale 1985):

Probability (either target hit in one radiation event) = 2 p R dt. (3.38)

Assuming that sub-lethal damage inflicted by such irradiation repairs exponentially with time constant μ, and at time t later:

$$\textit{Probability (damage still exists)} = 2 * p * \mathrm{R} * exp\left(-\mu t\right) dt\,. \tag{3.39}$$

Accordingly, total probability of inflicting sub-lethal damage in time t is (Dale 1985):

$$= 2pR\int_0^t exp\left(-\mu t\right) dt\,, \tag{3.40}$$

$$= \frac{2pR}{\mu}\left[1 - exp\left(-\mu t\right)\right]. \tag{3.41}$$

In addition, at any time the probability of a second target being hit in time dt is:

$$= pRdt\,. \tag{3.42}$$

Hence, assuming that ε is the interaction probability between two sub-lethally damaged targets, the total probability of lethal damage per target pair following irradiation of duration time T as derived by Dale (1985):

$$= 2\varepsilon p^2 R^2 \int_0^T t dt \,, \tag{3.43}$$

$$= \varepsilon p^2 R^2 T^2 \,. \tag{3.44}$$

If n is assigned as number of target pairs and the total acute dose given (D) is equal to RT, then, total Type B damage is (Dale 1985):

$$= n\varepsilon p^2 R^2 T^2 \,, \tag{3.45}$$

$$= \beta D^2 \,, \tag{3.46}$$

where, $$\beta = n\varepsilon p^2 \,. \tag{3.47}$$

Type A damage which is directly proportional to dose is given by $\alpha RT = \alpha D$.

Since it is assumed that sub-lethal damage repairs exponentially with a time constant μ for protracted irradiation, and the existing probability of sub-lethal damage at time t is defined as equation (3.31), type B damage may be fully expressed as reported by Dale (1985):

$$Type\ B\ Damage = \frac{2R^2\beta}{\mu}\left\{T - \frac{1}{\mu}\left[1 - exp\left(-\mu T\right)\right]\right\}. \tag{3.48}$$

Therefore, $$RE_{Protracted} = 1 + \frac{\frac{2R^2\beta}{\mu}\left\{T - \frac{1}{\mu}\left[1 - exp\left(-\mu T\right)\right]\right\}}{\alpha RT}, \tag{3.49}$$

$$RE_{Protracted} = 1 + \frac{2R}{\mu}\left(\frac{\beta}{\alpha}\right)\left\{1 - exp\left(-\mu T\right)\right\}. \tag{3.50}$$

For extended radiation treatments with a decaying source (e.g. Iridium-192 in High-Dose-Rate Brachytherapy or HDR-BT) a concept similar to the protracted irradiation case above applies except that the second hit contributing to Type B damage might be occurring at a dose rate which is lower (for fast decaying sources

such as Iridium-192) than that which produced the first hit. In addition, as the treatment proceeds, the probability of any event taking place reduces exponentially. Hence, the average *RE* over an extended period (*T*) of irradiation is given by (Dale 1985):

$$RE_T = 1 + \frac{2R_0\lambda}{\mu\text{-}\lambda}\left(\frac{\beta}{\alpha}\right) * \left[1 - exp(-\lambda T)\right]^{-1} * \left\{\frac{1}{2\lambda}\left[1 - exp(-2\lambda T)\right] - \frac{1}{\mu+\lambda}\left[1 - exp\left\{-T(\mu+\lambda)\right\}\right]\right\}, \tag{3.5}$$

where, R_0 is the initial dose rate and λ is the radioactive decay constant.

In the case of a permanent radioactive seed implant (e.g. I-125 Low-Dose-Rate Brachytherapy or LDR-BT) when time *T* is infinitely large, *RE* may be defined as proposed by Dale (1985):

$$RE_\infty = 1 + \frac{2R_0\lambda}{\mu-\lambda}\left(\frac{\beta}{\alpha}\right)\left[\frac{1}{2\lambda} - \frac{1}{\mu+\lambda}\right], \tag{3.52}$$

then,
$$RE_\infty = 1 + \frac{R_0}{\mu+\lambda}\left(\frac{\beta}{\alpha}\right). \tag{3.53}$$

In conclusion, the physical doses defined in DVHs from different radiation treatment schedules (fractionation schemes) can be converted to doses ($BE_{ff}D$) associated with specific biological end-points by multiplying the physical doses with the *RE* factor assigned to the specific dose fractionation scheme. As a result, $BE_{ff}D$-based DVHs ($BE_{ff}DVHs$) of different radiation treatment schedules normalised to the same biological end-point (for the particular organ/tissue) can be generated. This is more representative of relevant clinical end-points in OARs when different treatment modalities are to be compared.

3.3.2 Equivalent Dose (D_{eq})

In combined-modality treatment of prostate cancer, different radiation treatment modalities, for example, External Beam Radiation Therapy (EBRT) and LDR-BT or HDR-BT, are used to deliver the therapeutic dose to the tumour target volume. In some cases these treatments are even combined. It is well recognized that the dose response relationship in radiation therapy is not linear but follows a Linear-Quadratic (LQ) function. Hence, doses delivered by different modalities cannot be added to each other to predict the effect of the combined-modality treatment (Nag and Gupta 2000). $BE_{ff}D$, as described in previous section, can be calculated to determine the dose contribution of each modality to a specific biological end-point. However, $BE_{ff}D$ is not based on the standard 2 Gy/fraction schedule and therefore not familiar to the clinician as a means of predicting various complications in the OARs resulting from exposure to $BE_{ff}D$. Accordingly, $BE_{ff}D$ is converted subsequently to a more familiar term of Equivalent Dose (D_{eq}). Equivalent dose is the $BE_{ff}D$ of a particular dose fractionation scheme calculated as though the dose is given as conventionally fractionated irradiation (2 Gy/fraction). Equivalent dose may be calculated from following the equation (Nag and Gupta 2000):

$$D_{eq} = \frac{BE_{ff}D}{\left(1 + \frac{d_{ref}}{\alpha/\beta}\right)}, \qquad (3.54)$$

where d_{ref} is the reference dose per fraction for a conventionally fractionated external beam treatment to be used for calculating the D_{eq} (normally 2 Gy/fraction). The expression therefore allows comparing different fractionation schemes and their respective NTCPs which are clinically meaningful.

In summary, in order to estimate critical normal tissue and OARs complications for different radiation treatment techniques for prostate cancer, differential DVHs of OARs such as rectum, bladder, urethra, and femoral heads were retrieved from actual treatment plans. The physical doses in the differential DVHs were converted to $BE_{ff}D$ and D_{eq} subsequently and model parameters then applied to D_{eq}-based differential DVHs to obtain NTCP. Two common NTCP models, the relative seriality and Lyman, were used in this thesis. Model parameters for each organ were obtained from published studies. Details of the involving radiation treatment techniques used for the studies and the derived differential DVHs, and NTCP estimates will be presented in the next chapter.